Bathymetric effect on the winter sea surface temperature and climate of the Yellow and East China Seas

Shang-Ping Xie,[1,2] Jan Hafner,[1] Youichi Tanimoto,[3,4] W. Timothy Liu,[5] Hiroki Tokinaga,[3] and Haiming Xu[1,6]

Received 15 July 2002; accepted 18 September 2002; published 28 December 2002.

[1] Whether and how the atmosphere reacts to changes in extratropical sea surface temperature (SST) is under intense debate and this lack of understanding has been a major obstacle in the study of non-El Nino climate variability. Using new satellite measurements, we detect clear ocean-to-atmospheric feedback in the Yellow and East China (YEC) Seas that is triggered by the submerged ocean bottom topography. Under intense surface cooling in winter, water properties are well mixed up to 100 m deep. Ocean depth thus has a strong influence on SST of the continental shelf, leading to a remarkable collocation of warm tongues and deep channels. High winds and increased cloudiness are found over these warm tongues; one such band of ocean-atmospheric co-variation meanders through the basin, following a deep channel for an amazing distance of 1000 km. In addition to these climatic effects, the Kuroshio Front—where the warm current meets the much colder shelf water—strengthens the growth of storms. *INDEX TERMS:* 3339 Meteorology and Atmospheric Dynamics: Ocean/atmosphere interactions (0312, 4504); 4243 Oceanography: General: Marginal and semienclosed seas. **Citation:** Xie, S., J. Hafner, Y. Tanimoto, W. T. Liu, H. Tokinaga, and H. Xu, Bathymetric effect on the winter sea surface temperature and climate of the Yellow and East China Seas, *Geophys. Res. Lett.*, *29*(24), 2228, doi:10.1029/2002GL015884, 2002.

1. Introduction

[2] The Yellow and East China (YEC) Sea is one of the largest shelf seas of the world (its 1.25 million km^2 area is twice the size of the North Sea). Supporting heavy shipping, fishing and oil-drilling activities, it has great economic and climatic importance for the half billion people living in its coastal regions. One climatic effect of the YEC Sea is readily illustrated by much warmer winter temperatures on its east than west coast. For example, January temperature is 6.4°C in Nagasaki (32.4°N), Japan, but only 3.7°C in Shanghai (31.3°N) on the continental side. Whether and how the SST in the YEC Sea has any significant effects on the regional climate beyond this land-sea thermal contrast is not known because until now there has been a lack of adequate observational data.

[3] Using the new satellite measurements of unprecedented time-space resolution [*Wentz et al.*, 2000; *Xie et al.*, 2001], we find that the submerged bottom topography triggers coherent interactions between SST and key climate variables such as surface wind, heat flux and cloud cover. Moreover, using a state-of-the-art atmospheric model, we show that the SST distribution of the YEC Sea significantly affects winter-storm development in the region, a result useful for weather forecast.

2. Data and Model

[4] We use the following datasets: SST, cloud water and precipitation measurements by Tropical Rain Measuring Mission (TRMM) satellite's microwave imager (TMI), available since December 1998 at 0.25° resolution [*Wentz et al.* 2000]; and scatterometer measurements of sea surface vector wind on the QuikSCAT satellite [*Liu*, 2002], available since July 1999 at 0.25° resolution.

[5] We use the Mesoscale Model version 5 (MM5) [*Grell et al.*, 1995], in a domain that extends from 117°E to 139°E, 21°N to 41°N. It has a horizontal resolution of 27 km and 22 sigma levels in the vertical, of which twelve are placed below $\sigma = 0.8$ or about 2 km above the ground to resolve the planetary boundary layer (PBL). The U.S. National Centers for Environmental Prediction four times daily analysis is used as the initial and lateral boundary conditions. The SST climatology based on Advanced Very High Resolution Radiometer (AVHRR) measurements for 1985-1999 at 9 km resolution [*Armstrong and Vazquez-Cuervo*, 2001] is used as surface boundary conditions.

3. Bathymetric Control of SST

[6] The Kuroshio Current is the western boundary current of the North Pacific subtropical gyre and exerts an important dynamic and thermal effect on the YEC Sea. It enters the YEC Sea east of Taiwan and exits south of Island of Yaku-shima (130.5°E, 30.5°N), Japan. Flowing on the shelf break in the YEC Sea, this current carries warm, saline water from the tropics and is visible as a weak warm tongue in the SST field between the continental shelf and Ryukyu Islands (Figure 1). In winter, the YEC Sea loses a huge amount of heat to the atmosphere as the northerly monsoonal wind brings in cold and dry air from the continent. As a result, a sharp SST front—the Kuroshio Front—forms between the warm Kuroshio and the cold shelf water.

[7] Most of the YEC Sea is less than 100 m deep. The winter SST field on the shelf displays rich structures. Off the Chinese coast, a warm tongue can be traced up to 31°N

[1]International Pacific Research Center, University of Hawaii, Honolulu, USA.
[2]Department of Meteorology, University of Hawaii, Honolulu, USA.
[3]Graduate School of Environmental Earth Science, Hokkaido University, Sapporo, Japan.
[4]Frontier Research System for Global Change, Yokohama, Japan.
[5]Jet Propulsion Laboratory, Pasadena, USA.
[6]Department of Atmospheric Sciences, Nanjing Institute of Meteorology, Nanjing, China.

0094-8276/02/2002GL015884$05.00

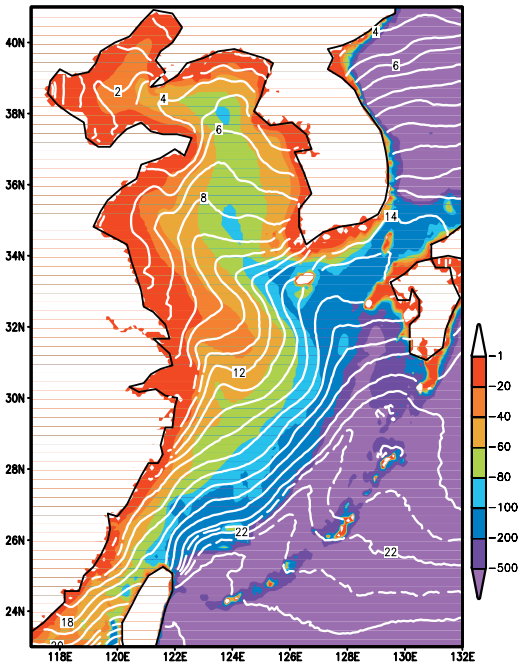

Figure 1. Bathymetry (color shade in m) and AVHRR SST climatology for January–March (contours at 1°C intervals) over the YEC Sea. The 21.5 and 22.5°C contours are dashed.

(Figure 1). A more pronounced warm tongue exists to the northeast, facing westward west of Cheju Island, Korea, and then pointing north in the Yellow Sea. Between these southwest and northeast warm tongues is a southeastward cold tongue. Previous studies attempted to link these tongue-like SST structures to advection by currents whose existence, however, has not been confirmed by direct measurements [see *Ichikawa and Beardsley* [2002] for a review].

[8] Here we propose an alternative mechanism that seems to explain the salient features of the SST climatology. Under intense winter cooling, the YEC Sea is well mixed in the upper 100 m [*Ichikawa and Beardsley*, 2002; *Chen et al.*, 1994]. Thus, the thermal inertia of a water column on the shelf is linearly proportional to the bottom depth, which determines the cooling rate of the water column. In other words, deep water cools much more slowly than shallow water and hence stays warmer. This one-dimensional bathymetric-control mechanism predicts a strong association between SST and bottom topography distributions. Indeed, the southwest warm tongue off the Chinese coast is collocated with a deep channel in 28–31°N, while the cold tongue to the northeast sits on a shallow bank. The main northeast warm tongue also follows a bathymetry trough. This close correlation between SST and bathymetry indicates that vertical mixing is the major mechanism determining the winter climatological SST distribution on the shelf north of 29°N and explains its departure from the general southward warming gradient expected from solar radiation.

[9] The net surface heat flux averaged over the YEC Sea and for October–March is about 200 Wm^{-2} [*Hirose et al.*, 1999; see also Figure 2C]. Under this surface forcing, the cooling rate is 5.2 °C/month for a water column 25 m deep but only 1.7 °C/month for a 75m column. Such a differential cooling over a 4-month period would yield a temperature difference of 14 °C between the 25 and 75 m isobaths, much greater than the observed SST difference. In reality, surface heat flux is a strong function of SST; colder water temperature over the shallow bank reduces the upward heat flux, providing a negative feedback onto the bathymetric effect.

[10] Horizontal advection seems to play a role in the SST distribution. Upon a closer inspection, there is a region of visible departure of SST from bathymetry in Figure 1, namely, the main warm tongue in the Yellow Sea is consistently shifted to the west of the bathymetry trough (~80 m deep), a possible effect of the westward Ekman advection. Alternatively, a northward flow on the western flank of the bathymetric trough and/or a southward flow near the Korean coast can cause this observed shift of the warm tongue. Because of insufficient in-situ observations, the Yellow Sea current system has not been reliably determined from direct measurements [*Ichikawa and Beardsley*, 2002], precluding a quantitative estimate of advection.

4. SST Effect on Wind and Clouds

[11] On seasonal average, the winter surface winds are northerly to northeasterly over the YEC Sea as part of the East Asian monsoon system (Figure 2c). The QuikSCAT wind speed shows a clear association with SST on the shelf, with high (low) wind speed observed over the warm (cold) tongue. In particular, the local wind speed maximum (minimum) we noted along the northeast warm (cold) tongue is unlikely to be due to orography on land because it is sufficiently far from the coast. To the south along the warmer flank of the Kuroshio Front, a wind speed maximum is located 100–200 km from the rather flat islands of Okinawa, again a likely effect of SST rather than orography. Analysis of historical ship reports confirms this SST modulation of surface wind speed (not shown). Nonaka and Xie [2003] report similar Kuroshio wind interaction further downstream south and east of Japan.

[12] SST variations affect the atmosphere through the following three mechanisms. First, a SST rise leads to a reduced static stability and hence stronger vertical mixing, which brings fast-moving air aloft down and accelerates the surface wind [*Hayes et al.*, 1989; *Xie et al.*, 1998]. Second, the SST increase warms the PBL by sensible and latent heat and forms an in-situ sea level pressure (SLP) low. The resultant SLP gradient causes wind adjustment [*Lindzen and Nigam*, 1987; *Hashizume et al.*, 2002]. Third, SST variations modulate the growth of extratropical storms (baroclinic instability), potentially leading to a deeper atmospheric response [*Inatsu et al.*, 2002]. We will return to this SST effect on storms in the later discussion.

[13] We use a high-resolution regional atmospheric model MM5 to study the mechanisms for these SST effects. The model integration starts on 1 February 2001 and lasts for a month. The monthly mean wind-speed field reproduces the satellite observations quite well, displaying a positive correlation with underlying SST (Figure 2b). The vertical mixing of momentum is the mechanism that underlies this positive SST-wind speed correlation. Indeed, surface sensible and latent heat fluxes, an important energy

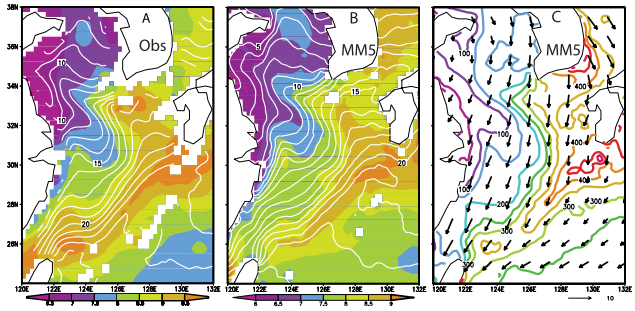

Figure 2. Scalar wind speed (color in m/s): (a) observed by QuickSCAT for January–March; and (b) simulated in MM5 for February 2001. (a) TRMM and (b) AVHRR SST climatologies are also plotted. (c) Surface turbulence heat flux (wm^{-2}) and wind velocity (ms^{-1}) in MM5.

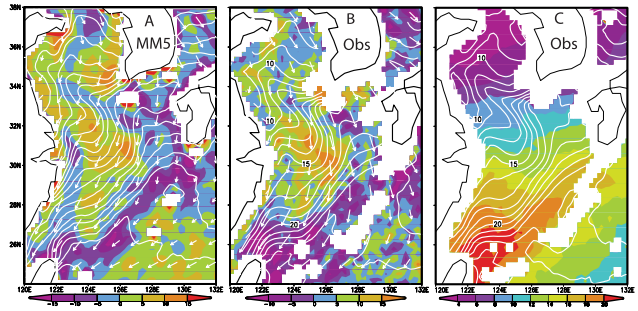

Figure 3. Surface wind divergence (10^{-6} s^{-1}): (a) in MM5 and (b) observed by QuikSCAT. (c) TMI cloud liquid water content climatology (10^{-2} mm) for January–March. SST is overlaid in white contours at 1°C intervals to show its correlations.

source for turbulent mixing in the PBL, is markedly enhanced over the warm tongues and the Kuroshio Front (Figure 2c). The flux amounts to about 100 Wm^{-2} off the Chinese coast but increases to 400 Wm^{-2} over the Kuroshio. The MM5 heat flux distribution is similar to that derived from ship observations [*Hirose et al.*, 1999], but shows a much more clear signature of warm and cold tongues because of model's high resolution.

[14] Another remarkable demonstration of SST-wind coupling is provided by the overlay of surface wind divergence on SST in MM5 (Figure 3a). Here the spatial derivative acts as a high-pass filter in favor of small horizontal scales. Wind convergence (divergence) is found near the warm (cold) tongue on the shelf and on the warmer (colder) flank of the Kuroshio Front. In particular, the wind convergence follows the main warm tongue that meanders from the southern tip of Kyushu Island all the way to the mouth of the Bohai Sea, over an amazing distance of more than 1,000 km. Upon closer inspection, wind convergence (divergence) tends to take place where the wind blows down- (up-) SST gradient over the YEC Sea, a phase relation consistent with vertical mixing [*Chelton et al.* 2001]. The wind divergence over the cold tongue on the shelf is an exception, despite wind blowing nearly along SST isolines—a phase relation consistent instead with the SLP mechanism.

[15] The wind divergence based on the QuikSCAT measurements (Figure 3b) is similar to that derived from the model, though somewhat noisier and less correlated with SST. This may indicate an overestimate of air-sea coupling in MM5 or alternatively, insufficient sampling by the QuikSCAT. The satellite scans a grid point only once or twice a day, a period during which a storm can travel across the YEC Sea.

[16] Furthermore, over the warmer part of the YEC Sea (south of 32°N), column-integrated cloud liquid water content measured by the TRMM satellite is markedly modulated by SST (Figure 3c). In particular, larger values of cloud water are observed on the warmer flank of the Kuroshio Front. Conversely, a reduction in cloud water in the mid-YEC Sea is found over the cold tongue. The precipitation distribution is very similar to that of cloud water (not shown). The moisture for greater precipitation over the warm tongues and the Kuroshio is supplied by surface wind convergence, which is highly correlated with SST (Figure 3).

5. Storm Development

[17] The atmosphere is highly variable over the winter YEC Sea, which is a preferred region for cyclone genesis [*Hanson and Long*, 1985]. Often, a weak atmospheric trough near Taiwan grows rapidly into a cyclone over the YEC Sea and then moves northeastward toward Japan. Called Taiwan cyclones in Japan, such storms threaten the safety of ship navigation and oil-drilling platforms in the YEC Sea, and bring high winds and sometimes snow to the Pacific coast of Japan.

[18] Extratropical storms grow on the large-scale horizontal air temperature gradient; their growth rate is proportional to the so-called baroclinicity defined as $\sigma = 0.31\frac{g}{T}|\nabla T|/N$, where g is the gravity, N the buoyancy frequency, and T air temperature [e.g., *Hoskins and Valdes*, 1990]. Taiwan cyclones are sub-synoptic (diameter~1,000 km), shallow surface depressions [*Chen et al.*, 1983] and may be influenced by the Kuroshio Front along which they travel.

[19] A Taiwan cyclone developed on 3–5 February 2001, which is captured in our MM5 simulation. At 18Z February 3, a weak surface low is found northeast of Taiwan (Figure 4a). It grows rapidly in the next 24 hours. At 18Z February

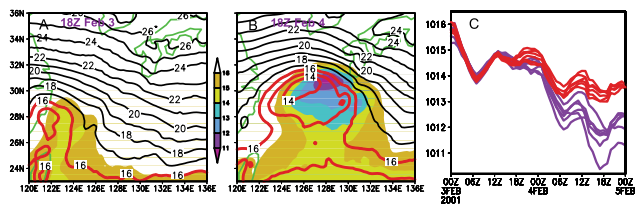

Figure 4. SLP-1000 (hPa): (a) at 18:00Z February 3 and (b) 24 hours later at 18:00Z February 4, 2001, in the MM5 simulations under high-resolution (color shade) and smoothed (contours) SST forcing. (c) The center pressure of the Taiwan cyclone in members of high-resolution (blue) and smoothed (red) SST ensembles. In (a) and (b), the model is initialized with the NCEP analysis at 12Z 31 January 2001.

4, it moves 1,000 km along the SST front to southwest of Kyushu Island and becomes a cyclone with several enclosed isobars (Figure 4b).

[20] To investigate the Kuroshio Front effect, we conduct two sets of ensemble simulations, one under the high-resolution AVHRR SST climatology for February and one under a smoothed version, horizontally averaged with a Gaussian weight at an e-folding scale of 2.8°. This smoothed SST dataset is similar to those used in operational weather forecast models, in which the Kuroshio Front is substantially weakened and the tongue-like structures on the shelf disappear all together. Except for this difference in SST, the two ensemble simulations are identical. In each ensemble, six integrations are made with initial conditions of the NCEP analysis at 12Z and 18Z January 31, 0Z, 6Z, 12Z and 18Z 1 February 2001, respectively.

[21] Figure 4c shows the time series of the Taiwan cyclone center pressures in the two sets of ensemble model runs. Initially, the lows in the two ensemble sets grow at a similar rate. While the center pressure levels off at 07Z February 4 in the smoothed SST runs, the cyclone continues to grow for the following 12 hours under the high-resolution SST runs. During this period, the center pressure in the smoothed SST runs almost always stays above that in the high-resolution SST runs. We interpret the difference in the cyclone growth as resulting from the large SST gradient across the Kuroshio Front, which controls the growth rate of baroclinic instability. Consistent with this interpretation, the intra-ensemble spread is larger in the high-resolution than in the smoothed SST ensemble because of the greater baroclinicity.

[22] In addition to increasing the local air temperature gradient, the Kuroshio Front helps set up a time-mean cross-frontal circulation that favors precipitation and latent heat release on its warmer flank. This precipitation and latent heat release further aid the growth of the cyclone by reducing the effective static stability, *N*. The rainband along the Kuroshio observed by satellites (Figure 3c) corroborates this latent heat effect.

6. Summary

[23] Ocean depth exerts a strong control over the winter SST distribution in the YEC Sea through intense vertical mixing that reaches 100 m deep. The deep channels and shallow banks on the continental shelf, therefore, lead to tongue-like warm and cold SST structures in the winter climatology. The continental break, furthermore, steers the Kuroshio Current, resulting in a strong SST front.

[24] On the continental shelf, wind speed and cloud water content are locally enhanced (reduced) over the warm (cold) tongue. On the warmer flank of the Kuroshio Front, we see a zone of high wind speeds and a band of raining cloud due to the region's unstable atmospheric stratification near the surface. In both the model and satellite observations, surface wind convergence is roughly collocated with the Kuroshio Current and over the warm SST tongues that meander through the YEC Sea for as far as 1,000 km. Finally we show that by increasing the baroclinicity and condensational heating, the Kuroshio Front aids the growth of the so-called Taiwan cyclone, an important winter weather phenomenon for Japan.

[25] **Acknowledgments.** The TMI and QuikSCAT data are obtained via ftp from Remote Sensing Systems and the AVHRR SST climatology from Jet Propulsion Laboratory. We thank G. Speidel for comments and M. Nonaka for helpful discussion. This work is supported by NASA through its QuikSCAT and TRMM missions and grant NAG5-10045, by Frontier Research System for Global Change, and by the Natural Science Foundation of China (40240420564). IPRC contribution number 176 and SOEST contribution number 6032.

References

Armstrong, E. M., and J. Vazquez-Cuervo, A new global satellite-based sea surface temperature climatology, *Geophys. Res. Lett.*, *28*, 4199–4202, 2001.

Chelton, D. B., et al., Observations of coupling between surface wind stress and sea surface temperature in the eastern tropical Pacific, *J. Climate*, *14*, 1479–1498, 2001.

Chen, C., R. C. Beardsley, R. Limeburner, and K. Kim, Comparison of winter and summer hydrographic observations in the Yellow and East China Seas and adjacent Kuroshio during 1986, *Cont. Shelf Res.*, *14*, 909–929, 1994.

Chen, T.-C., C.-B. Chang, and D. J. Perkey, Numerical study of an AMTEX '75 oceanic cyclone, *Mon. Wea. Rev.*, *111*, 1818–1829, 1983.

Grell, G., J. Dudhia, and D. Stauffer, A Description of the Fifth-Generation Penn State/NCAR Mesoscale Model (MM5). *NCAR Tech. Note, 398*, 122 pp., 1995.

Hanson, H. P., and R. Long, Climatology of cyclogenesis over the East China Sea, *Mon. Wea. Rev.*, *113*, 697–707, 1985.

Hashizume, H., et al., Direct observations of atmospheric boundary layer response to slow SST variations over the eastern equatorial Pacific, *J. Climate*, *15*, 3379–3393, 2002.

Hayes, S. P., M. J. McPhaden, and J. M. Wallace, The influence of sea surface temperature on surface wind in the eastern equatorial Pacific, *J. Climate*, *2*, 1500–1506, 1989.

Hirose, N., H.-C. Lee, and J.-H. Yoon, Surface heat flux in the East China Sea and the Yellow Sea, *J. Phys. Oceanogr.*, *29*, 401–417, 1999.

Hoskins, B. J., and P. J. Valdes, On the Existence of Storm-Tracks, *J. Atmos. Sci.*, *47*, 1854–1864, 1990.

Ichikawa, H., and R. C. Beardsley, The current system in the Yellow and East China Seas, *J. Oceanogr.*, *58*, 77–92, 2002.

Inatsu, M., H. Mukougawa, and S.-P. Xie, Tropical and extratropical SST effects on the midlatitude storm track, *J. Meteor. Soc. Japan*, *80*, 1069–1076, 2002.

Lindzen, R. S., and R. S. Nigam, On the role of sea surface temperature gradients in forcing low level winds and convergence in the tropics, *J. Atmos. Sci.*, *44*, 2418–2436, 1987.

Liu, W. T., Progress in scatterometer application, *J. Oceanogr.*, *58*, 121–136, 2002.

Nonaka, M., and S.-P. Xie, Co-variations of sea surface temperature and wind over the Kuroshio and its extension: Evidence for ocean-to-atmospheric feedback, *J. Climate*, *16*, in press, 2003.

Wentz, F. J., C. Gentemann, D. Smith, and D. Chelton, Satellite measurements of sea surface temperature through clouds, *Science*, *288*, 847–850, 2000.

Xie, S.-P., M. Ishiwatari, H. Hashizume, and K. Takeuchi, Coupled ocean-atmospheric waves on the equatorial front, *Geophys. Res. Lett.*, *25*, 3863–3866, 1998.

Xie, S.-P., W. T. Liu, Q. Liu, and M. Nonaka, Far-reaching effects of the Hawaiian Islands on the Pacific Ocean-atmosphere system, *Science*, *292*, 2057–2060, 2001.

S.-P. Xie, J. Hafner, and H. Xu, International Pacific Research Center, University of Hawaii, 1680 East West Road, Honolulu, HI 96822, USA. (xie@hawaii.edu)

Y. Tanimoto and H. Tokinaga, Graduate School of Environmental Earth Science, Hokkaido University, Sapporo 060-0810, Japan.

W. T. Liu, Jet Propulsion Laboratory 300–323, Pasadena, CA 91109-8099, USA.